



Diagnosing osteomyelitis in diabetic foot by diffusion-weighted imaging and dynamic contrast material-enhanced magnetic resonance imaging: a systematic review and meta-analysis

W. Wudhikulprapan^a, P. Phinyo^{b,c}, A. Hadi^d, T. Kanthawang^{a,*},
H.N. Choudur^d

^a Department of Radiology, Faculty of Medicine, Chiang Mai University, Thailand

^b Department of Family Medicine, Faculty of Medicine, Chiang Mai University, Chiang Mai, Thailand

^c Center for Clinical Epidemiology and Clinical Statistics, Faculty of Medicine, Chiang Mai University, Chiang Mai, Thailand

^d Department of Radiology, McMaster University, Hamilton, Ontario, Canada

ARTICLE INFORMATION

Article history:

Received 16 February 2024

Accepted 21 July 2024

AIM: To evaluate the diagnostic performance of diffusion-weighted imaging (DWI) and dynamic contrast enhanced (DCE), for diagnosing osteomyelitis in the diabetic foot.

MATERIALS AND METHODS: A thorough search was carried out to identify suitable studies published up to September 2023. The quality of the studies involved was evaluated using Quality Assessment of Diagnostic Accuracy Studies-2 (QUADAS-2). The diagnostic sensitivity and specificity of each imaging modality/method for each specific cut point were summarized. The summary receiver operating characteristic (SROC) curve was calculated using bivariate mixed effects models.

RESULTS: Five studies investigating 187 patients and 234 bone lesions with 110 diagnosed osteomyelitis were enrolled. Four studies used DWI (172 lesions), three studies used DCE techniques (140 lesions) and two studies presented results of conventional MRI (66 lesions). The sensitivity ranges using conventional MRI, DWI and DCE were 65%-100%, 65%-100% and 64%-100%, respectively. The specificity ranges were 50%-61%, 56%-95%, and 66%-93%, respectively. The SROC curve of DWI and DCE was 0.89 (95% CI, 0.86–0.92) and 0.90 (95% CI, 0.87–0.92), respectively.

CONCLUSION: Combining DWI and DCE methods, alongside conventional MRI, can improve the reliability and accuracy of diabetic foot osteomyelitis diagnosis. However, the study recognizes result variability due to varying protocols and emphasizes the need for well-designed studies with standardized approaches. To optimize diagnostic performance, the study recommends considering low ADC values, Ktrans or rapid wash-in rate from DCE such as iAUC60, along with using large ROIs that cover the entire lesion while excluding normal bone marrow.

* Guarantor and correspondent: T. Kanthawang, Department of Radiology Faculty of Medicine, Chiang Mai University, 110 Intavaroros Rd, Sriphum, Meung Chiang Mai 50200, Thailand.

E-mail addresses: wanat_w@cmu.ac.th (W. Wudhikulprapan), phichayutphinyo@gmail.com (P. Phinyo), ayeshahadi@hotmail.com (A. Hadi), thanatkanthawang@gmail.com (T. Kanthawang), hnalnic@yahoo.com (H.N. Choudur).

<https://doi.org/10.1016/j.crad.2024.07.015>

0009-9260/© 2024 The Royal College of Radiologists. Published by Elsevier Ltd. All rights are reserved, including those for text and data mining, AI training, and similar technologies.

Introduction

Individuals with long-term diabetes and peripheral neuropathy face increased foot complications, especially when combined with vascular issues. Diabetics have up to a 34% lifetime incidence of foot ulcers, with a 60% recurrence rate within 3 years.¹ Half of diabetic foot wounds are clinically infected at presentation.² These infections often lead to diabetic foot osteomyelitis (DFO), requiring antibiotics and sometimes surgery.³ Inadequate treatment can result in foot amputation or septicemia. DFO is a major cause of non-traumatic lower-extremity amputations and is linked to a 30% 5-year mortality rate.⁴ Prompt identification and treatment are essential. DFO often coexists with Charcot neuropathy (CN), requiring careful differential diagnosis for effective management.

Blood tests, including white blood cell count, C reactive protein (CRP), and erythrocyte sedimentation rate (ESR), are initial steps to detect osteomyelitis.⁵ Positive results typically trigger further diagnostic tests. The definitive diagnosis involves histopathology or microbiological analysis of bone biopsy or pus. However, biopsies are invasive, require anesthesia, and analysis takes several days.

Foot imaging enhances DFO diagnostics and minimizes unnecessary biopsies. Techniques include plain radiographs, ultrasound, computed tomography (CT) scans, planar scintigraphy, magnetic resonance imaging (MRI) scans, bone scintigraphy including white blood cell (WBC) scan, positron emission tomography (PET) scans, and single-photon emission computed tomography (SPECT).^{3,6,7} Recent meta-analyses,^{6,7} have highlighted the high diagnostic accuracy of conventional MRI in identifying DFO. MRI, recommended after an initial radiograph, is endorsed by NICE and ACR.^{8,9} However, MRI's varying specificity may lead to potential osteomyelitis overdiagnosis.

Advances in MR imaging, such as higher magnetic field strength and improved coil design, facilitate advanced techniques for diabetic foot assessment. Diffusion-weighted imaging (DWI) detects water diffusion in tissues, aiding in osteomyelitis, bone marrow edema, and abscess detection. Dynamic contrast-enhanced (DCE) MR imaging assesses microvascular characteristics. Although common in tumor assessments, these techniques are underused in diabetic foot evaluations despite their benefits.¹⁰

DWI is notable in musculoskeletal imaging for its sensitivity, specificity, and no need for contrast media, beneficial for diabetic patients with renal issues. However, diverse protocols yield varied DFO detection results in DWI and DCE studies. These techniques are analyzed qualitatively, semi-quantitatively, or quantitatively.^{11,12} Our meta-analysis evaluated DW-MRI and DCE-MRI's diagnostic value in DFO, providing guidance on their use.

Materials and methods

Evidence acquisition

This systematic review followed the Centre for Reviews and Dissemination (CRD) guidance and the Preferred Reporting Items for Systematic Review and Meta-analysis (PRISMA) protocol. Ethical board approval was exempted (RAD-2566-0632).

Search strategy and study selection

Systematic searches were independently conducted in PubMed, Scopus, and Embase by two musculoskeletal radiologists with 3 and 9 years of experience (W.W. and T.K., respectively). Searches were performed in September 2023. The search keywords were as follows: for “diabetic foot” AND “foot osteomyelitis” AND (“nuclear magnetic resonance imaging” AND “diffusion weighted imaging” AND “dynamic contrast-enhanced magnetic resonance imaging”) with no language, date, geographical or study design restrictions. Both free-text words and Medical Subject Headings terms were used in the search strategy involving “All Fields” (Table 1). The reviewers also performed a manual search through the references of various articles as well as a search for unpublished and ongoing studies in the [ClinicalTrials.gov](https://www.clinicaltrials.gov) database.

Included studies assessed MRI with DWI and/or DCE against histopathology for suspected DFO. Controls were patients without infection confirmed clinically and through imaging. Criteria for inclusion were studies with at least five patients, excluding reviews and case reports. Studies using conventional MRI without DCE and DWI were also excluded to allow a direct comparison of diagnostic performance. Discrepancies in study selection were resolved by a third reviewer with 20 years of experience (H.N.C.).

Table 1

Search terms used for Embase, Scopus and Pubmed.

Database	Keyword
Embase	(“Diabetic foot”/exp OR “diabetic feet” OR “diabetic foot” OR “diabetic foot syndrome” OR “diabetic foot ulcer” OR “foot ulcer, diabetic” OR “diabetic foot osteomyelitis”/exp OR “foot osteomyelitis”/exp) AND (“nuclear magnetic resonance imaging”/exp OR “diffusion weighted imaging”/exp OR “dynamic contrast-enhanced magnetic resonance imaging”/exp)
Scopus:	(TITLE-ABS-KEY (diabetic AND foot) AND TITLE-ABS-KEY (magnetic AND resonance AND imaging) OR TITLE-ABS-KEY (diffusion AND weighted AND imaging) OR TITLE-ABS-KEY (dynamic AND contrast-enhanced AND magnetic AND resonance AND imaging) AND TITLE-ABS-KEY (osteomyelitis) OR TITLE-ABS-KEY (ulcer))
Pubmed	((((diabetes mellitus) AND (Foot ulcer)) AND (osteomyelitis)) OR (diffusion weighted imaging)) AND (dynamic contrast-enhanced magnetic resonance imaging)

Data extraction

Data from selected articles were extracted using forms, including author, publication year, country, study type, patient data, number of lesions, reference standards, and MRI techniques. The first reviewer extracted data, which was then verified independently by the second. Analysis included patients with histopathologic confirmation post-MRI and those in the non-infection group based on clinical and imaging follow-up. True-positive, false-positive, true-negative, and false-negative results were used to estimate diagnostic accuracy indices per study. The diagnostic accuracy of MRI types, including DWI and DCE-MRI, in detecting DFO was assessed. Two reviewers independently used the QUADAS-2 tool to assess the risk of bias in individual studies.¹³

Statistical analyses

All statistical analyses were performed using statistical software (Stata, version 14.2, Stata Corp). Due to the significant methodological heterogeneity among each imaging modality, we did not pool the reported diagnostic indices. The area under the summary receiver operating characteristic curve (SROC AUC) was generated to assess the summary accuracy of DWI and DCE.¹⁴ Heterogeneity among studies was assessed using I^2 statistics.

Results

Patient, study, and MRI characteristics

Following a systematic search of databases, we identified a total of 3,486 articles: 1869 from PubMed, 928 from Scopus, 672 from Embase and 17 articles from manual search through the references of published articles. After screening the titles and abstracts and eliminating duplicate records, we assessed a total of 591 articles for eligibility. Ultimately, five articles met the inclusion criteria, constituting a cohort comprising 187 patients and 234 bone lesions, with 110 of these lesions being diagnosed as DFO^{15–19} (Fig 1). Among five studies, four specifically involved diabetic patients with clinical and laboratory indications of acute osteomyelitis. The study by Kruk *et al.* focused on patients referred for forefoot MRI, without explicitly stating their diabetic status.¹⁷ Nevertheless, we included this study in our meta-analysis because it targeted bone lesions, and diabetic patients comprised the majority of pedal osteomyelitis cases.

All the included studies were prospective investigations conducted at various institutions, utilizing positive histological and/or microbiological analyses as the reference standard for diagnosing osteomyelitis. Among these five articles, which employed bone marrow edema in the control group for comparison, four studies utilized acute neuropathic arthropathy as the control group. In these four studies, the control group was diagnosed through negative bone biopsy¹⁹ or based on imaging criteria in two studies,^{16,18} or diagnosis by exclusion in one study.¹⁵ In another study, degenerative or stress-related alterations

within the bone marrow edema group were used as controls. In this case, the control group was identified as those without clinical suspicion of infection either at the time of imaging or during clinical follow-up.¹⁷

The mean of the mean ages of the patients in the evaluable articles was 56.65 years (range, 22–89 years). There was male predominance (59.89%). Osteomyelitis is common in forefoot (metatarsal bone) and calcaneus while non-osteomyelitis condition is more common in mid foot (around navicular, cuboid, and cuneiform bones). The characteristics of the individual articles are shown in detail in Table 2.

Four studies utilized DWI (comprising 172 lesions),^{15–17,19} while three studies employed DCE techniques (comprising 140 lesions)^{16,18,19} and two studies presented the results of conventional MRI (comprising 66 lesions).^{15,19} Of the two studies that presented results of conventional MRI, one study interpreted only non-contrast study,¹⁵ while the other employed both pre- and post-contrast MRI.¹⁹ Both studies were interpreted by a single musculoskeletal radiologist using prespecified criteria for identifying MRI-positive cases of DFO. These two articles utilized a common criterion of focal abnormal signal intensity in the bone marrow, and only one study incorporated a subtending skin ulcer into its criteria.¹⁵

In terms of region of interest (ROI) placement in DWI and DCE, as shown in Table 2. Three studies employed unfixed circular ROIs within the bone lesion,^{15,17,19} one study used a fixed ROI size (ranging from 35 to 45 mm²),¹⁸ and another study utilized both a small circular ROI and a manually drawn ROI outlining the entire bone lesion.¹⁶ Across all included studies, ROIs were carefully positioned within the lesions, avoiding the adjacent normal bone marrow to prevent inaccurate apparent diffusion coefficient (ADC) values.

In three of five articles, image analysis involved two independent musculoskeletal radiologists who were blinded to clinical information, and interobserver agreement was calculated.^{15–17} Diez *et al.* reported moderate interobserver agreement for time intensity curve (TIC) and small ROI for DWIr, K^{trans} and $iAUC_{60}$ (Table 2). However, the large ROI in Diez *et al.*'s study and other two studies exhibited good to excellent agreement. In another study, image interpretation was based on the consensus of two musculoskeletal radiologists who were also blinded to clinical information.¹⁸ Additionally, in one study, MRI analysis was performed by a single musculoskeletal radiologist prior to undergoing bone biopsy.¹⁹

In the four DWI studies, a consistent use of the same MRI vendor was observed, predominantly with 1.5T machines rather than 3.0T. Specifically, two studies utilized only 1.5T MRI machines,^{15,16} one employed a 3T machine,¹⁹ and another study used both 1.5T and 3T machines.¹⁷ Detailed DWI protocols for each article are available in Table 3. All four studies relied on mean ADC values, with one study¹⁶ additionally utilizing the high b-value signal pathological-to-normal bone ratio (DWIr). Notably, in Diez *et al.*'s study, DWIr derived from a freehand ROI encompassing the entire bone lesion showed statistical significance, whereas

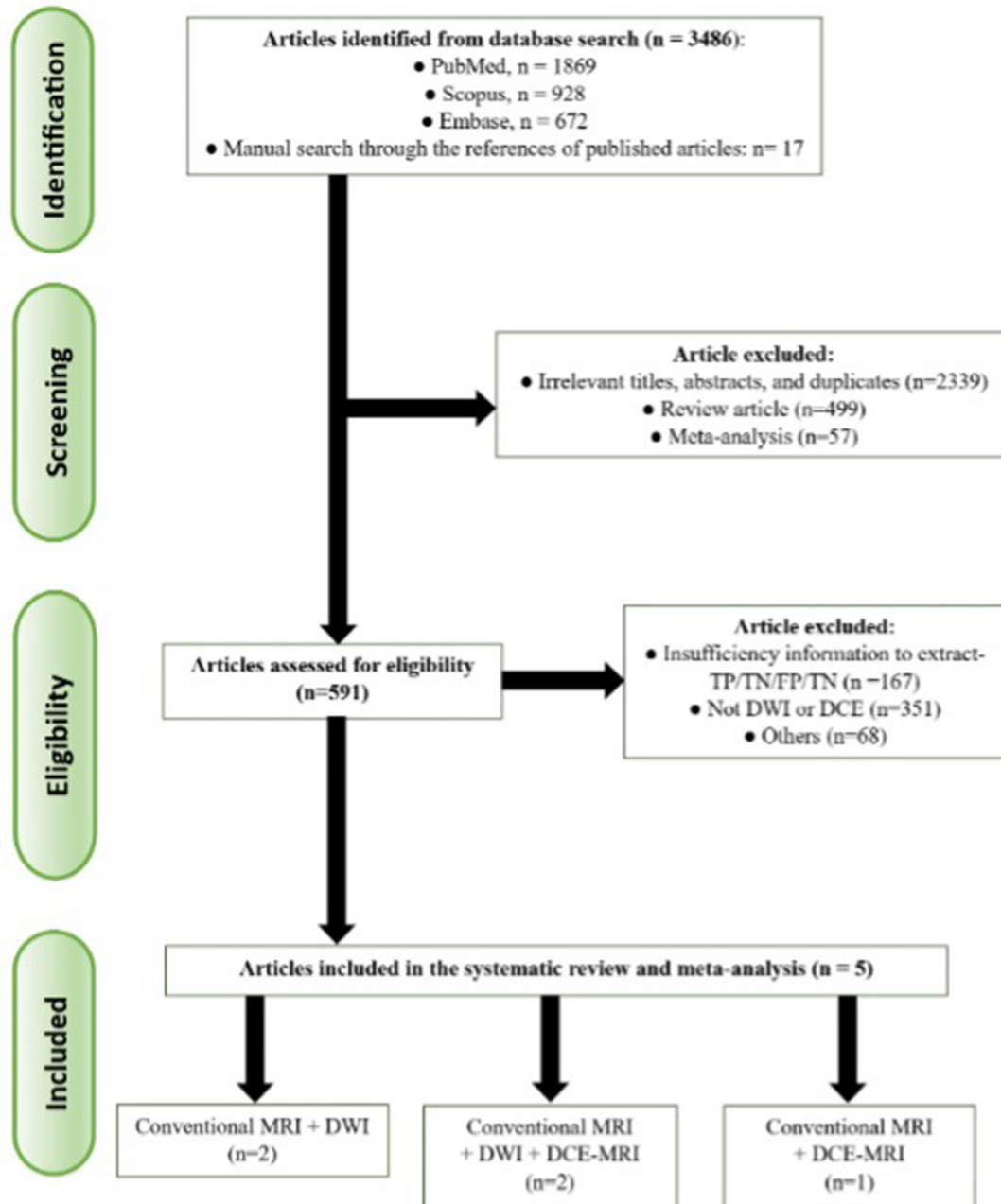


Figure 1 Flow diagram showing the study selection process for the meta-analysis.

mean ADC values from both small circular ROIs and free-hand ROIs did not.¹⁶ Qualitative assessments were not employed in any of the evaluable studies. Across all studies, the ADC values for osteomyelitis were consistently lower than those for the bone marrow edema group,^{15,16,19} except for Kruk *et al.*'s study, where the ADC value in the osteomyelitis group was higher than in the bone marrow edema group.¹⁷ Each study subsequently conducted ROC analysis to define cutoff values for ADC.

DCE MRI provides various assessment methods, including qualitative, semiquantitative, and quantitative approaches. In the three DCE studies, two incorporated

quantitative assessments, utilizing pharmacokinetic models to derive parameters such as the volume transfer constant (K^{trans}), the volume of contrast material returning to the vascular compartment (K_{ep}), and extracellular volume (V_e).^{16,18} The other two studies employed qualitative assessment, focusing on TIC pattern.^{16,19} For semi-quantitative assessment, one study used SI_0 , SI_{max} , SI_{rel} , wash in rate (WIR), time to peak,¹⁹ while another study used iAUC60 (16). Detailed DCE protocols for each article are provided in Table 4. Diez *et al.*'s study demonstrated statistical significance for K^{trans} and iAUC60 from both small circular and freehand ROIs but not for other parameters. Raj

Table 2
Baseline characteristics of the included studies.

Authors	Year	Country	Study types	NO. of patients (M/F)	Age (years) mean \pm SD or median (range)	NO. lesions (OM/non-infection)	Reference standard for OM	Comparison	MRI techniques	ROI placement	Diffusion parameters evaluated	DCE parameters evaluated
Abdel Razek AAK	2017	Egypt	Prospective	41 (22/19)	51 (48–72)	23/18	HP ^a	Acute CN	Conventional MRI (No contrast) + DWI	Within the abnormal areas avoiding the adjacent normal BM	Mean ADC value	-
Kruk KA	2022	Switzerland	Prospective	60 (33/27)	For OM; 68.5 \pm 11.0 (49–90), For BME; 53 \pm 18.5 (22–89)	20 OM/ 20 BME	HP ^a	Degenerative or stress-related alterations	Conventional MRI (with contrast) + DWI	Circular ROI within the target bone lesion	Mean ADC value	-
Diez AIG	2020	Spain	Prospective	31 (22/9)	57 (36–82)	18 (18 patients)/ 50 (14 patients)	HP ^a	Acute CN	Conventional MRI (with contrast) + DWI + DCE-MRI + FDG-PET	One small ROI and another covering bone lesion as large as possible	mean ADC values, DWI ^b	K^{trans} , K_{ep} , V_e , $iAUC_{60}$, TIC and TIC patterns (1–V) ^c
Raj S	2022	India	Prospective	25 (17/8)	52.5 \pm 7.4	19/6	HP ^a	Acute CN with negative bone biopsy	Conventional MRI (with contrast) + DWI + DCE-MRI	ROI over bone lesion (15–40 mm ²)	Mean ADC value	SI_0 , SI_{max} , SI_{rel} , wash in rate [WIR], time to peak, mean TIC, TIC pattern (1–3) ^d
Liao D	2018	China	Prospective	30 (18/12)	57.92 \pm 12.3	30/30	HP ^a	Acute CN	Conventional MRI (with contrast) + DCE-MRI	ROIs were fixed in size (35–45 mm ²)	-	K^{trans} , K_{ep} , V_e ^c

NO.: Number; M/F: male/female; ROI: Region of interest; NA: Not applicable; DM: Diabetes mellitus; OM: Osteomyelitis; MRI: Magnetic resonance imaging; DWI: Diffusion weighted imaging; ADC: Apparent diffusion coefficient; HP: histopathology; BM: bone marrow; BME: bone marrow edema; CN: Charcot neuro-arthropathy; DCE: Dynamic contrast material-enhanced; FDG-PET: fluorodeoxyglucose-positron emission tomography.

^a HP stands for histological and/or microbiological analysis.

^b DWI^r means high b-value signal pathological-to-normal bone ratio.

^c The extended Tofts model and population-averaged arterial input function (AIF) were used on DCE-MRI to obtain a volume transfer constant [K^{trans} ; related to wash-in], reflux rate [K_{ep} ; related to washout], volume fraction of the extravascular-extracellular matrix/space [V_e], internal area under the gadolinium curve at 60 s [$iAUC_{60}$], and time-intensity curve (TIC). The shape of the TIC was classified according to the model described by Rijswijk *et al.* [23] (TIC I to V). TIC patterns I or II were defined as CN and patterns III, IV or V as OM (denominated TIC_{model}) [15,24].

^d SI_0 = tissue signal intensity on unenhanced T1 images; SI_{max} = maximum absolute contrast enhancement; maximum relative SI [SI_{rel}] = ($SI_{max} - SI_0$)/ $SI_0 \times 100$; wash in rate [WIR] = ($SI_{max} - SI_0$)/time to peak in seconds; time to peak (T) = time taken to reach the maximum signal intensity in seconds. The mean TIC of the lesion was also analysed to characterize the lesion. Three patterns of the TIC were considered, type 1 – progressive increase in signal intensity over the entire dynamic study (the persistent pattern), type 2 – rapid initial peak followed by a relative constant enhancement (the plateau pattern), and type 3 – sharp uptake of contrast followed by a decrease in enhancement over time (the washout pattern).

Table 3
Imaging parameters of included studies with DWI.

Authors	Year	MRI vendors	Strength (T)	Coil	Plane	Sequence type	b-values (s/mm ²)	TR/TE (msec)	Matrix size	Slice thickness (mm)*	FOV (mm)	NEX	Others
Abdel Razek AAK	2017	Symphony, Siemens	1.5	Extremity coil	Axial	Multi-slice, single-shot, echo-planar	0, 400, 800	10,000/108	256 × 128	3	160–200	4	Bandwidth = 300 KHz, interslice gap=1 mm
Kruk KA	2022	Magnetom Skyra, Magnetom Vida, Magnetom Avanto fit and Magnetom Aera, Siemens	1.5, 3 (21/19)	NA	Sagittal	Readout-segmented echo-planar	0, 50, 800	4280/70 (1.5T), 4100/69 (3T)	110 × 110 (1.5T), 160 × 160 (3T)	NA	150 × 150 (1.5T), 160 × 160 (3T)	4	- At b-value = 50; 1 (1.5T), 10 (3T) - At b-value = 800; 3 (1.5T), 36 (3T)
Diez AIG	2020	Aera; Siemens	1.5	Extremity coil	Coronal	Inversion recovery single-shot spin-echo planar	0, 800	11,000/127	128 × 128	5	272 × 272	4	Inversion recovery delay = 180 msec, sensitivity encoding factor=2 Voxel size (1.7 × 1.3 × 5 mm)
Raj S	2022	TIM Magnetom Verio, Siemens	3	Extremity coil	Axial	Single-shot echo-planar	0, 600, 800	4100/90	NA	5	250	NA	

T: Tesla; NA: Not applicable; TR/TE repetition time/echo time; FOV: Field of view; NEX: number of excitations; NA: Not applicable; msec: millisecond; mm: millimeter.

et al.'s study found statistical significance for SI_0 , SI_{rel} , and WIR . Liao *et al.*'s study showed statistical significance for K^{trans} and V_e .

Quality assessment of studies

Most studies had a generally low overall risk of bias assessed by the QUADAS-2 tool (Fig 2). However, Kruk *et al.*'s study included patients without a specified diagnosis of diabetic foot,¹⁷ while the other studies enrolled patients consecutively and had a low risk of bias in patient selection. Four out of five studies ensured blinding of MRI interpretation to bone biopsy results, except for Raj *et al.*, which lacked this information.¹⁹ Histopathology was uniformly used as the reference standard for diagnosing osteomyelitis, but only one study¹⁹ employed it for diagnosing CN. Kruk *et al.* did not specify the non-infection group's composition,¹⁷ and Diez *et al.* did not follow up on non-infection cases to confirm the diagnosis.¹⁶ Diez *et al.*'s study uniquely provided the time interval between MRI and surgery in DFO cases.¹⁶ Overall, the studies exhibited a low concern regarding applicability in patient selection, index test, and reference standard, except for patient selection in Kruk *et al.*'s study¹⁷ and the index test in Raj *et al.*'s study.¹⁹

Diagnostic accuracy of MRI for osteomyelitis

The results of the five articles were aggregated for the evaluation of diagnostic test accuracy (Table 5). Due to differences in the techniques used for the interpretation of DWI and DCE, we decided not to pool the results. The sensitivity ranges for the detection of osteomyelitis using conventional MRI, DWI, and DCE were 65%–100% (with lower and upper confidence intervals of 45% to 100%), 65%–100% (43% to 100%), and 64%–100% (35% to 100%), respectively (Fig 3). The specificity ranges for the detection of DFO using conventional MRI, DWI, and DCE were 50%–61% (with lower and upper confidence intervals of 19% to 81%), 56%–95% (42% to 99%), and 66%–93% (30% to 98%), respectively (Fig 3). The SROC AUC for DWI and DCE was 0.89 (95% CI, 0.86–0.92) and 0.90 (95% CI, 0.87–0.92), respectively (Figs 4 and 5). Unfortunately, the AUC of conventional MRI cannot be calculated due to the limited number of studies.

Measures of heterogeneity

The included studies were clinically heterogeneous with respect to the study design, activity administered, and criteria for determination of test positivity. Substantial statistical heterogeneity was noted for the pooled AUC estimate of DWI and DCE ($I^2 = 68\%$ and 52%), respectively.

Subgroup analyses

Subgroup analyses were conducted to assess sensitivity and specificity based on the criteria used for DWI interpretation. The three studies utilizing the mean ADC value reported a sensitivity range of 65%–95% (with lower and upper confidence intervals of 43% to 99%) and a specificity range of 70%–95% (44% to 99%).^{15,17,19} The cutoff values for

Table 4
Imaging parameters of included studies with DCE-MRI.

Authors	Year	MRI vendors	Strength (T)	Coil	Sequence type	Contrast injection	TR/TE (msec)	Matrix size	Slice thickness (mm)	FOV (mm)	Acquisition time ^a	Others ^b
Diez AIG	2020	Aera, Siemens	1.5	Extremity coil	fat-saturated 3D VIBE sequence in the axial plane	Images were obtained after a bolus injection of 0.1 mmol gadobutrol (Gadovist; Bayer) per kg of body weight and a 20-ml saline flush at a rate of 2.0 ml/s.	3.3–3.6/1.3	256 × 215	1.5	220 × 110	240 s with 10 s per frame	Intersection gap=0.3, flip angle 10
Raj S	2022	TIM Magnetom Verio, Siemens	3	Extremity coils	VIBE sequence	A dose of 0.2 mmol/kg of gadolinium chelate (Magnevist/gadopentate dimeglumine) was administered at a rate of 3.5 ml/s followed by a chaser injection of 20–30 ml of normal saline given at the same rate.	4.1/1.4	NA	3	170	A temporal resolution of 15–16 s over 4–5 minutes post-injection of contrast.	12 serial axial images; voxel size of 0.7 × 0.7 × 0.6 mm
Liao D	2018	GE	3	8-channel phased-array head coil	NA	A dose of 0.1 mmol/kg Gd-DTPA (gadodiamide) was injected and acquired using an automatic double-bolus injection at a rate of 2 ml/s, followed by a 20-ml saline flush at the same rate.	6.1/2.9	256 × 160	4	180 × 180	A total of 35 frames were acquired; the total DCE-MRI acquisition time ranged from 210 to 230 s	Spatial resolution = 2 × 1.2 × 6.0 mm, bandwidth = 31.25 kHz, and flip angle = 10°

T: Tesla; NA: Not applicable; S: Seconds; TR/TE repetition time/echo time; FOV: Field of view; VIBE: Volumetric interpolated breath-hold examination; mmol: millimole; kg: kilogram; ml: milliliter; mm: millimeter; msec: millisecond; s: second; kHz: kilohertz.

^a Temporal resolution dynamic acquisition every 3–5 sec at least 5 min to evaluate washout.

^b Parallel imaging minimal sense factor of 2.

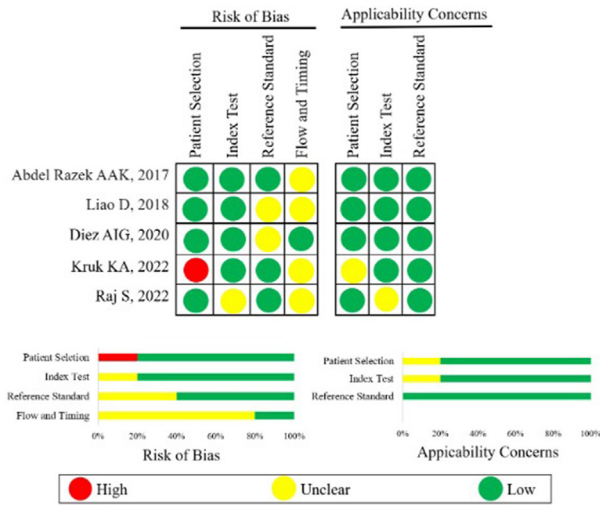


Figure 2 Summary of the risk of bias and applicability concerns across the included studies as assessed with QUADAS-2 forms.

mean ADC ranged from 0.98 to $1.57 \times 10^{-3} \text{ mm}^2/\text{s}$, with a mean value of $1.21 \times 10^{-3} \text{ mm}^2/\text{s}$. The SROC AUC for mean ADC was 0.92 (95% CI, 0.89–0.94). Furthermore, one study employing DWIr with two independent reviewers demonstrated a sensitivity range of 72%–100% (49% to 100%) and a specificity range of 56%–78% (42% to 87%).¹⁶ The cutoff values for DWIr were 4.15 and 5.12.

Discussion

Studies evaluating the diagnostic value of DWI and DCE for DFO are scarce. This meta-analysis demonstrates that DWI and DCE exhibit good diagnostic performance for distinguishing between DFO and bone marrow edema in diabetic foot, with increased specificity compared to conventional MRI (Fig 6). To the best of our knowledge, this meta-analysis is the first to systematically compare advanced techniques, namely DWI and DCE, with conventional MRI to evaluate the diagnostic performance in detecting osteomyelitis in cases of diabetic foot. This information can guide the consideration of functional MRI before

Table 5 Diagnostic results of MRI parameters for osteomyelitis and non-infection.

First author [Reference no.]	Parameters	Cut-off value	Total number of bone lesions (DFO/non-infection)	TP	FP	FN	TN	Sensitivity (%)	Specificity (%)	Value in osteomyelitis Mean ± SD (95%CI) or median (IQR) ^d	Value in non-infection Mean ± SD (95%CI) or median (IQR) ^d
Conventional MRI											
Abdel Razek ¹⁵	Non-contrast study	-	23/18	15	7	8	11	65.2	61.1	-	-
Raj ¹⁹	Pre- and post-contrast study	-	19/6	19	3	0	3	100	50.0	-	-
Diffusion weighted MRI											
Abdel Razek ¹⁵	Mean ADC ^a	<0.98	23/18	20	3	3	15	87.0	83.3	0.86 ± 0.11 (0.73–1.3)	1.27 ± 0.19 (0.82–1.47)
		<1.04	23/18	19	1	4	17	82.6	94.4	0.85 ± 0.12 (0.74–1.35)	1.26 ± 0.21 (0.82–1.47)
Kruk ¹⁷		>1.234	20/20	16	4	4	16	80.0	80.0	1.432 ± 0.222 (1.082–1.918)	1.071 ± 0.196 (0.599–1.388)
		>1.155	20/20	19	6	1	14	95.0	70.0		
		>1.32	20/20	13	1	7	19	65.0	95.0		
Raj ¹⁹		<1.57	17/6	15	1	2	5	88.2	83.3	1.35 ± 0.24 (NA)	1.64 ± 0.14 (NA)
Diez ¹⁶	DWIratio	>4.15	18/50	18	22	0	28	100	56.0	5.80 (4.51–6.97) ^d	3.82 (2.33–5.51) ^d
		>5.12	18/50	13	11	5	39	72.2	78.0	4.96 (4.65–6.50) ^d	3.84 (2.40–5.07) ^d
Dynamic contrast enhanced MRI											
Diez ¹⁶	K ^{transb}	>0.09	11/44	9	11	2	33	81.8	75.0	0.14 (0.08–0.20) ^d	0.06 (0.05–0.10) ^d
		>0.11	11/44	8	7	3	37	72.7	84.1	0.15 (0.07–0.20) ^d	0.07 (0.04–0.09) ^d
Liao ¹⁸		>0.11	30/30	24	2	6	28	80.0	93.3	0.819 ± 1.172 (NA)	0.025 ± 0.029 (NA)
Liao ¹⁸	Ve ^b	>0.19	30/30	24	2	6	28	80.0	93.3	0.483 ± 0.328 (NA)	0.101 ± 0.054 (NA)
Diez ¹⁶	iAUC60 ^c	>3.23	11/44	11	15	0	29	100	65.9	7.02 (3.98–11.09) ^d	2.19 (0.84–5.18) ^d
		>5.69	11/44	7	7	4	37	63.6	84.1	7.02 (3.54–11.94) ^d	2.19 (0.76–4.21) ^d
Raj ¹⁹	Mean SI ₀	>143.30	19/6	18	1	1	5	94.7	83.3	199.45 ± 33 (NA)	132.68 ± 44 (NA)
	SI _{max}	>408.35	19/6	17	2	2	4	89.5	66.7	470.5 ± 34 (NA)	376.01 ± 86 (NA)
	Mean WIR	>1.21	19/6	16	1	3	5	84.2	83.3	2.08 ± 0.4 (NA)	0.932 ± 0.2 (NA)

DFO: Diabetic foot osteomyelitis; TP: true-positive; FP: false-positive; FN: false-negative; TN: true-negative; SD: Standard deviation; IQR: interquartile range; ADC: Apparent Diffusion Co-efficient; DWIr: signal of the pathological-to-normal bone ratio in the b800 DWI; K^{trans}: volume transfer constant; Kep: reflux rate; Ve: volume fraction of the extravascular extracellular matrix; iAUC₆₀: internal area under the gadolinium curve at 60 seconds; SI₀: tissue signal intensity on unenhanced T1 images; SI_{max} = maximum absolute contrast enhancement; WIR (wash in rate) = (SI_{max} – SI₀)/time to peak in seconds = .

^a ADC value presents in $\times 10^{-3} \text{ mm}^2/\text{s}$.

^b K^{trans} and Ve presents in millimeter/minute.

^c iAUC₆₀: internal area under the gadolinium curve at 60 s presents in mmol contrast minute.

^d median (IQR).

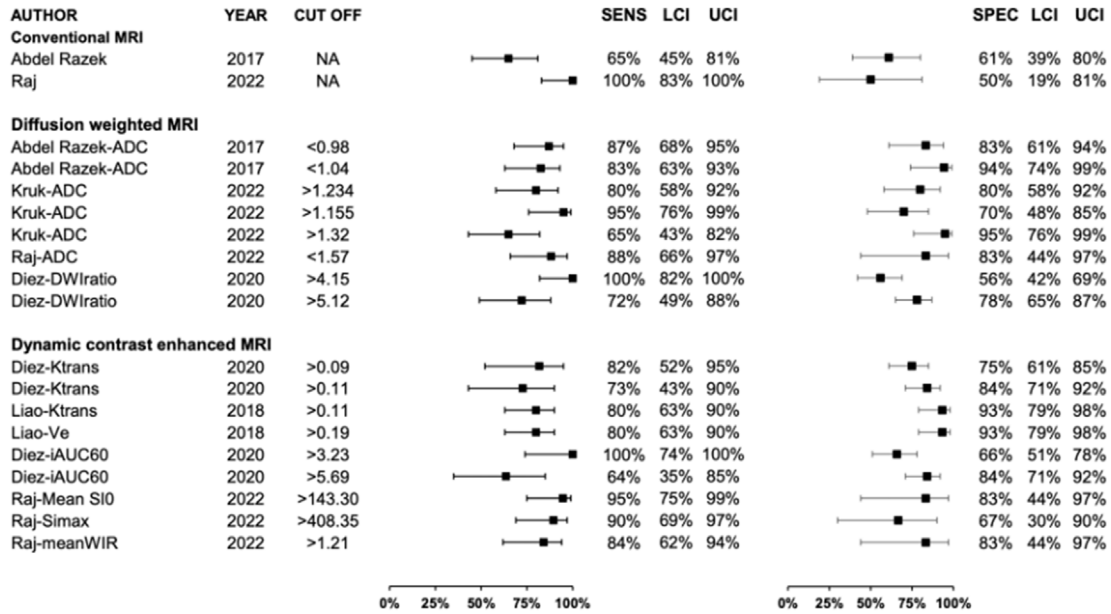


Figure 3 Reported diagnostic sensitivity and specificity of conventional MRI, ADC values derived from DWI and parameters derived from dynamic contrast enhanced study.

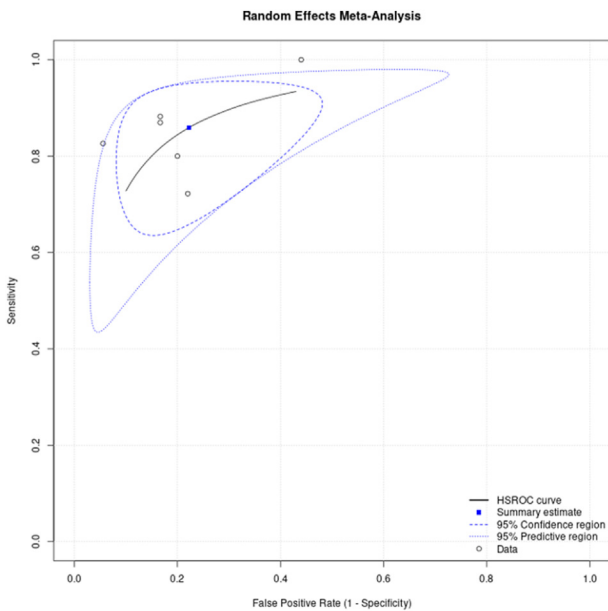


Figure 4 Summary receiver operating characteristics (sROC) curve of diagnostic performance of ADC values derived from DWI. The pooled AUC estimate for DWI was 0.89 (95%CI = 0.86–0.92) with an $I^2 = 68%$ and Q value of 6.25.

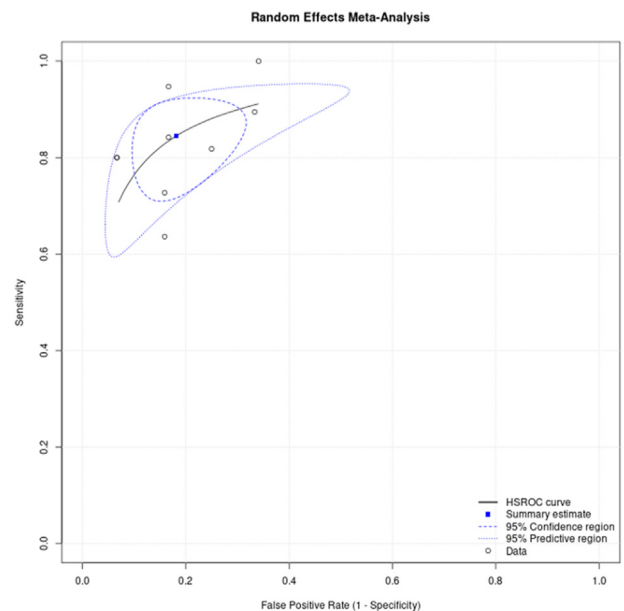


Figure 5 Summary receiver operating characteristics (sROC) curve of diagnostic performance of parameters derived from dynamic contrast enhanced study. The pooled AUC estimate was 0.90 (95% CI = 0.87–0.92) with an $I^2 = 52%$ and Q value of 4.13.

resorting to nuclear medicine techniques such as ^{18}F -FDG PET/CT or WBC scan.

Recent meta-analysis on DFO diagnosis focus on conventional MRI, which shows high sensitivity (96.4%) but moderate specificity (83.8%), compared to PET’s 92.8% specificity.⁶ This suggests a risk of false positives with MRI. Clinicians and radiologists should be cautious of overdiagnosis, especially in surgical cases. Our study found that

conventional MRI has similar sensitivity but lower specificity (50%–61%) compared to Llewellyn *et al.*’s 76.0%–89.5%.⁶ This may be due to different DFO diagnostic criteria in the studies reviewed.^{15,19} Lower specificity could relate to secondary infection signs needed to distinguish CN from infection, especially in the mid-foot. These signs include periosteal reaction, skin ulcers, sinus tracts, cellulitis, abscesses, and foreign bodies.²⁰ Only one study considered

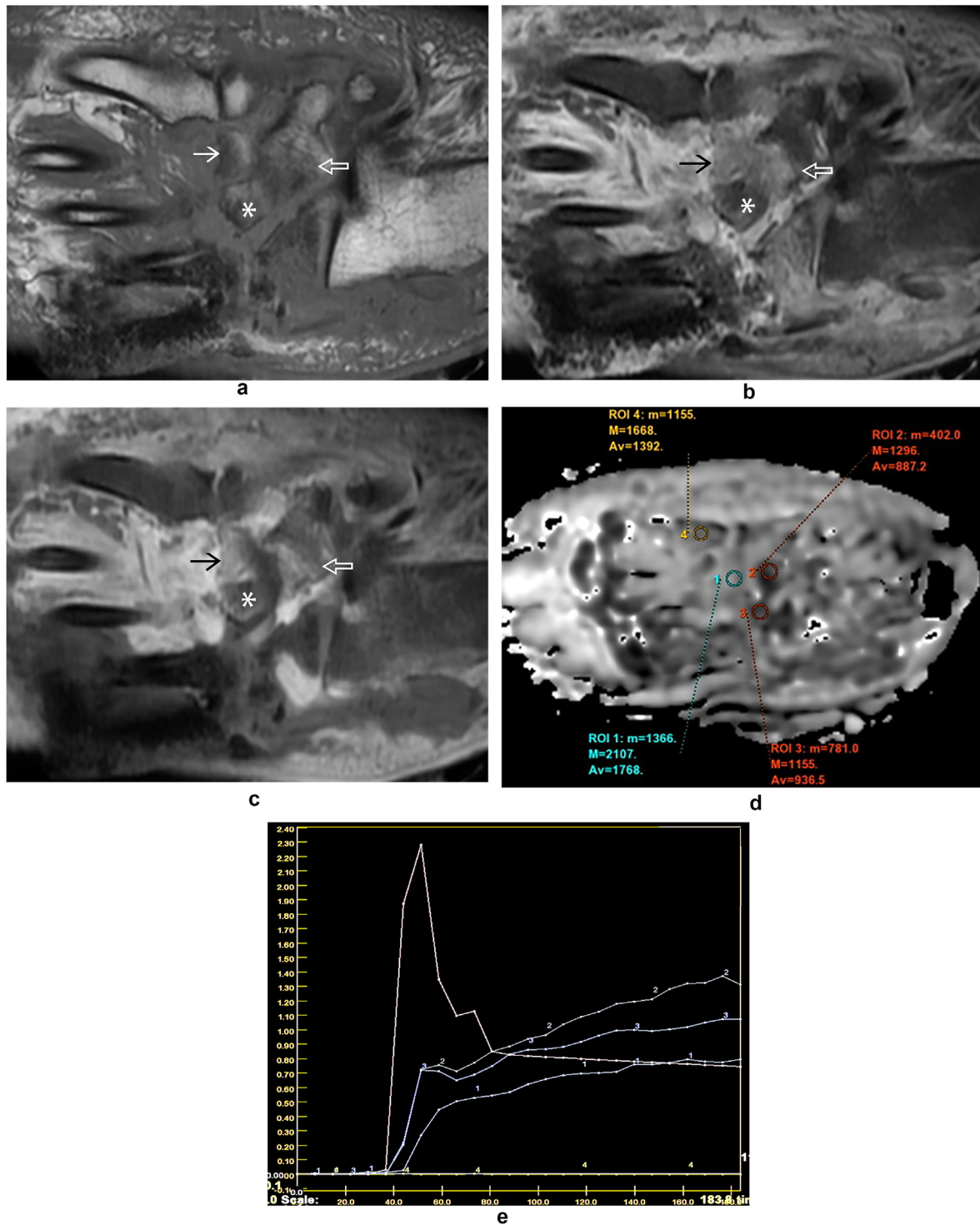


Figure 6 A 46-year-old man with diabetes mellitus and foot ulcer. Axial (a) T1-WI, (b) T2-WI with FS, and (c) CE T1-WI with FS show abnormal bone marrow signal in the midfoot bones (arrow = intermediate cuneiform, open arrow = navicular, and asterisk = lateral cuneiform bones). (d) ADC map of abnormal bone marrow in the intermediate cuneiform (ROI1), navicular (ROI2) and lateral cuneiform (ROI3) bones, and normal 1st metatarsal bone (ROI4). The average ADC values were 1.77, 0.89, 0.94, and $1.39 \times 10^{-3} \text{ mm}^2/\text{sec}$, respectively. (e) DCE showing TIC from ROI same as in (d) showed rapid initial enhancement followed by sustained late enhancement in the navicular (ROI2) and lateral cuneiform (ROI3) bones but slow progressive enhancement in the intermediate cuneiform bone (ROI1) compared to non-enhancement in the normal metatarsal bone (ROI4). The K^{trans} values from the same ROI measured 0.09, 0.2, and 0.4, N/A mL/min, respectively. ADC and DCE were suggestive of osteomyelitis in the lateral cuneiform and navicular bones but reactive bone marrow in the intermediate cuneiform, which was confirmed by biopsy and follow-up MRI.

WI, weighted image; FS, fat suppression; CE, contrast enhanced; ADC, apparent diffusion coefficient; ROI, region of interest; DCE, dynamic contrast enhanced study; TIC, time intensity curve; N/A, not accessible.

these criteria. However, our study's pooled specificity for DWI and DCE remains higher than the recent meta-analysis.⁶

Bone marrow abnormalities often lead to higher ADC values.^{12,17} In diabetic patients, CN and osteomyelitis-related bone marrow edema coexist.²¹ CN shows elevated DWI signal and higher ADC values due to the T2 shine-through effect, while osteomyelitis typically has higher DWI signal but intermediate ADC values, reflecting water diffusion restriction.¹² Although most studies report lower ADC values in osteomyelitis,^{15,19,22} Kruk *et al.* found higher ADC values in osteomyelitis than in stress or degenerative conditions.¹⁷ Variability in ADC values in DFO is due to complex bone marrow signals on DWI and ADC maps, influenced by factors like inflammatory infiltration, bone infarction, purulence in osteomyelitis, and red marrow contamination.^{12,23,24}

Overlapping mean ADC values in studies^{15–17,19} likely due to shared factors such as increased blood flow and capillary leakage in both CN and DFO. ADC cutoff values vary considerably, ranging from 0.98 to 1.57×10^{-3} mm²/s, consistent with previous review²⁴ which lack consensus on the optimal ADC measurements. Diez *et al.* introduced DWIr, comparing DWI values between pathological and normal bone, showing higher values in DFO. This method has been effective in conditions like pancreatic cysts and bone marrow-replacing lesions such as multiple myeloma and metastasis.^{25,26} Prior reviews have favored minimal ADC values for better diagnostic performance in soft tissue masses, offering insights into cellular composition, as mean ADC values can be diluted by myxoid, cystic, or less cellular regions within the ROI.²⁷ However, further comprehensive validation is warranted.

Several technical factors influencing the heterogeneity of ADC values in studies should be considered. Firstly, variations in magnetic field strengths (e.g., 1.5 T and 3 T) can introduce bias, as seen in phantom studies,²⁸ impacting reported ADC values. Secondly, the choice of diffusion imaging methods can influence outcomes. For instance, the utilization of readout-segmented echo-planar imaging (rs-EPI), as in Kruk *et al.*'s study, offers advantages in image quality compared to standard single-shot echo-planar imaging (ss-EPI), which is susceptible to artifacts.^{17,29} Thirdly, normal bone marrow ADC values may vary slightly based on anatomical locations, ranging from 0.2 to 0.5×10^{-3} mm²/sec.³⁰ For instance, healthy forefoot bone reported by Kruk *et al.* exhibited an ADC value of 0.28×10^{-3} mm²/sec, with a range from 0.14 to 0.47×10^{-3} mm²/sec. Finally, to enhance the separation of ADC values, employing more b-values or incorporating a non-zero minimum b-value (>100 s/mm²), as suggested in prior research,^{12,31} may be beneficial. Higher b-values in diffusion-weighted imaging scans have been proposed for obtaining ADC values with a lower effect of blood perfusion and a better representation of water molecule diffusion within the tissue.³²

Conventional post-contrast imaging lacks microcirculation details, while DCE MRI offers various assessment methods. For the quantitative approach, there were a few disparities in K_{ep} and V_e , while two studies found higher

K^{trans} values in osteomyelitis, identifying a cutoff of >0.11 mL/min for distinguishing DFO from CN.^{16,18} This may be due to increased abnormal vessel density, blood flow, and permeability. Liao *et al.* highlighted that, among all DCE-MRI parameters, K^{trans} exhibited stronger correlations with CRP levels and ESR than other parameters. These results emphasize the significance of K^{trans} as a key parameter for diagnosing DFO.

Standardization issues in DCE sequence design and postprocessing limit quantitative assessment's routine use. For diabetic foot assessment, qualitative and semi-quantitative methods namely wash in rate ([maximum signal intensity (SI)–SI at unenhanced T1 weighted image]/time to peak in seconds) and iAUC60 (internal area under the gadolinium curve at 60 second) are often sufficient, showing diagnostic accuracy comparable to K^{trans} .^{16,19} DFO-induced hyperemia and vasodilation increase capillary transudation, leading to rapid contrast uptake and higher wash-in rates. However, semi-quantitative variables are sensitive to variations in acquisition protocols and hardware settings, challenging study comparisons. iAUC60, derived from the signal intensity curve, is becoming popular in soft tissue tumors due to its robustness and contrast-medium independence.^{33,34}

Qualitative assessment using the TIC lacks consensus in DCE analysis, with varying TIC classifications in two available studies.^{16,19} However, notable findings emerge. Firstly, no washout pattern is observed in DFO and CN cases. This pattern is common in tumor.³⁵ Secondly, the absence of an enhancement pattern or the presence of slow progressive enhancement in the TIC (indicating a slow wash-in rate) suggests CN over DFO. Lastly, DFO usually shows rapid initial enhancement followed by a plateau phase or sustained late enhancement, reflecting the presence of an inflammatory process with recirculation and contrast agent leakage. This points out that a further careful examination of the pattern of TIC may provide differentiation between DFO and CN in future research.

Several other important considerations exist in functional MRI studies. ROI placement significantly affects ADC values and DCE parameters, with larger ROIs performing better.¹⁶ We recommend using ROIs covering the entire lesion while excluding normal bone marrow. Additionally, red and yellow marrow proportions impact ADC values and DCE measurements. Red marrow has higher ADC values and perfusion due to increased vascularity and hematopoietic activity.^{12,36} Red marrow exhibits higher ADC values (0.68×10^{-3} mm²/sec; range $0.61–0.74 \times 10^{-3}$ mm²/sec) compared to yellow marrow (0.38×10^{-3} mm²/sec; range $0.31–0.44 \times 10^{-3}$ mm²/sec).²⁵ Yellow marrow shows minimal signal changes on DCE. Understanding this marrow composition is crucial for interpreting DWI and DCE results. Some propose using chemical shift or Dixon imaging with ADC analysis to distinguish bone marrow edema from infections in diabetic foot cases.¹² Age, vascular supply, and osteoporosis may also influence perfusion, potentially affecting DCE results.³⁷

This meta-analysis has limitations. The number of included studies was small, and only two provided data on

DFO detection using conventional MRI alone.^{15,19} This restricts assessing the additional diagnostic value of advanced MRI techniques. The studies varied in MRI interpretation criteria, vendors, sequences, and disease physiologies, affecting conclusions. Therefore, more standardized studies are needed to confirm DCE and DWI's effectiveness in DFO detection.

Conclusion

This study suggests that combining DWI and DCE methods, alongside conventional MRI, can improve the reliability and accuracy of diabetic foot osteomyelitis diagnosis. However, it also acknowledges the limited number of studies, result variability due to varying protocols, and emphasizes the necessity for well-designed studies with larger patient cohorts and standardized approaches. To optimize diagnostic performance, the study recommends considering low ADC values, K^{trans} or rapid wash-in rate from DCE such as $iAUC_{60}$, along with using large ROIs that cover the entire lesion while excluding normal bone marrow.

Funding

This research was partially supported by Chiang Mai University.

Authors contribution

Thanat Kanthawang and Hema Nalini Choudur take responsibility for the integrity of the work as a whole, from inception to finished article.

Conception and design of the study: Kanthawang, Phinyo, Hadi, Choudur.

Acquisition of data: Kanthawang, Wudhikulprapan.

Analysis and interpretation of data: Kanthawang, Phinyo, Choudur.

Drafting of article or revising it critically for important intellectual content: Kanthawang, Wudhikulprapan, Phinyo, Choudur.

Final approval of the version of the article to be published: Kanthawang, Wudhikulprapan, Phinyo, Hadi, Choudur.

Conflict of interest

The authors declare no conflict of interest.

Acknowledgments

None.

References

- Armstrong DG, Boulton AJM, Bus SA. Diabetic foot ulcers and their recurrence. *N Engl J Med* 2017;**376**:2367–75.
- Lipsky BA, Aragon-Sanchez J, Diggle M, et al. IWGDF guidance on the diagnosis and management of foot infections in persons with diabetes. *Diabetes Metab Res Rev* 2016;**32**:45–74.
- Carek PJ, Dickerson LM, Sack JL. Diagnosis and management of osteomyelitis. *Am Fam Physician* 2001;**63**:2413–20.
- Brennan MB, Hess TM, Bartle B, et al. Diabetic foot ulcer severity predicts mortality among veterans with type 2 diabetes. *J Diabetes Complications* 2017;**31**:556–61.
- Lima AL, Oliveira PR, Carvalho VC, et al. Diretrizes Panamericanas para el Tratamiento de las Osteomielitis e Infecciones de Tejidos Blandos G. Recommendations for the treatment of osteomyelitis. *Braz J Infect Dis* 2014;**18**:526–34.
- Llewellyn A, Kraft J, Holton C, et al. Imaging for detection of osteomyelitis in people with diabetic foot ulcers: a systematic review and meta-analysis. *Eur J Radiol* 2020;**131**:109215.
- Lauri C, Tammimga M, Glaudemans A, et al. Detection of osteomyelitis in the diabetic foot by imaging techniques: a systematic review and meta-analysis comparing MRI, white blood cell scintigraphy, and FDG-PET. *Diabetes Care* 2017;**40**:1111–20.
- National Institute for Health and Care Excellence: Guidelines. *Diabetic foot problems: prevention and management*. London: National Institute for Health and Care Excellence (NICE); 2019. Copyright © NICE 2019.
- Expert Panel on Musculoskeletal I, Walker EA, Beaman FD, et al. ACR appropriateness criteria(R) suspected osteomyelitis of the foot in patients with diabetes mellitus. *J Am Coll Radiol* 2019;**16**:S440–50.
- Vilanova JC, Baleato-Gonzalez S, Romero MJ, et al. Assessment of musculoskeletal malignancies with functional MR imaging. *Magn Reson Imaging Clin N Am* 2016;**24**:239–59.
- Padhani AR. Diffusion magnetic resonance imaging in cancer patient management. *Semin Radiat Oncol* 2011;**21**:119–40.
- Martín Noguero T, Luna Alcalá A, Beltrán LS, et al. Advanced MR imaging techniques for differentiation of neuropathic arthropathy and osteomyelitis in the diabetic foot. *Radiographics* 2017;**37**:1161–80.
- Whiting PF, Rutjes AW, Westwood ME, et al. QUADAS-2: a revised tool for the quality assessment of diagnostic accuracy studies. *Ann Intern Med* 2011;**155**:529–36.
- Harbord RM, Whiting P, Sterne JA, et al. An empirical comparison of methods for meta-analysis of diagnostic accuracy showed hierarchical models are necessary. *J Clin Epidemiol* 2008;**61**:1095–103.
- Abdel Razek AAK, Samir S. Diagnostic performance of diffusion-weighted MR imaging in differentiation of diabetic osteoarthropathy and osteomyelitis in diabetic foot. *Eur J Radiol* 2017;**89**:221–5.
- Diez AIG, Fuster D, Morata L, et al. Comparison of the diagnostic accuracy of diffusion-weighted and dynamic contrast-enhanced MRI with (18)F-FDG PET/CT to differentiate osteomyelitis from Charcot neuro-osteoarthropathy in diabetic foot. *Eur J Radiol* 2020;**132**:109299.
- Kruk KA, Dietrich TJ, Wildermuth S, et al. Diffusion-weighted imaging distinguishes between osteomyelitis, bone marrow edema, and healthy bone on forefoot magnetic resonance imaging. *J Magn Reson Imaging* 2022;**56**:1571–9.
- Liao D, Xie L, Han Y, et al. Dynamic contrast-enhanced magnetic resonance imaging for differentiating osteomyelitis from acute neuropathic arthropathy in the complicated diabetic foot. *Skeletal Radiol* 2018;**47**:1337–47.
- Raj S, Prakash M, Rastogi A, et al. The role of diffusion-weighted imaging and dynamic contrast-enhanced magnetic resonance imaging for the diagnosis of diabetic foot osteomyelitis: a preliminary report. *Pol J Radiol* 2022;**87**:e274–80.
- Donovan A, Schweitzer ME. Use of MR imaging in diagnosing diabetes-related pedal osteomyelitis. *Radiographics* 2010;**30**:723–36.
- Ahmadi ME, Morrison WB, Carrino JA, et al. Neuropathic arthropathy of the foot with and without superimposed osteomyelitis: MR imaging characteristics. *Radiology* 2006;**238**:622–31.
- Eren MA, Karakaş E, Torun AN, et al. The clinical value of diffusion-weighted magnetic resonance imaging in diabetic foot infection. *J Am Podiatr Med Assoc* 2019;**109**:277–81.
- Urish KL, Cassat JE. Staphylococcus aureus osteomyelitis: bone, bugs, and surgery. *Infect Immun* 2020;**88**.
- Kumar Y, Khaleel M, Boothe E, et al. Role of diffusion weighted imaging in musculoskeletal infections: current perspectives. *Eur Radiol* 2017;**27**:414–23.

25. Padhani AR, van Ree K, Collins DJ, et al. Assessing the relation between bone marrow signal intensity and apparent diffusion coefficient in diffusion-weighted MRI. *AJR Am J Roentgenol* 2013;**200**:163–70.
26. Inan N, Arslan A, Akansel G, et al. Diffusion-weighted imaging in the differential diagnosis of cystic lesions of the pancreas. *AJR Am J Roentgenol* 2008;**191**:1115–21.
27. Ahlawat S, Fayad LM. Diffusion weighted imaging demystified: the technique and potential clinical applications for soft tissue imaging. *Skeletal Radiol* 2018;**47**:313–28.
28. Lavdas I, Miquel ME, McRobbie DW, et al. Comparison between diffusion-weighted MRI (DW-MRI) at 1.5 and 3 tesla: a phantom study. *J Magn Reson Imaging* 2014;**40**:682–90.
29. Porter DA, Heidemann RM. High resolution diffusion-weighted imaging using readout-segmented echo-planar imaging, parallel imaging and a two-dimensional navigator-based reacquisition. *Magn Reson Med* 2009;**62**:468–75.
30. Dietrich O, Biffar A, Reiser MF, et al. Diffusion-weighted imaging of bone marrow. *Semin Musculoskelet Radiol* 2009;**13**:134–44.
31. Khoo MM, Tyler PA, Saifuddin A, et al. Diffusion-weighted imaging (DWI) in musculoskeletal MRI: a critical review. *Skeletal Radiol* 2011;**40**:665–81.
32. Zong RL, Geng L, Wang X, et al. Diagnostic performance of apparent diffusion coefficient for prediction of grading of pancreatic neuroendocrine tumors: a systematic review and meta-analysis. *Pancreas* 2019;**48**:151–60.
33. Breault SR, Heye T, Bashir MR, et al. Quantitative dynamic contrast-enhanced MRI of pelvic and lumbar bone marrow: effect of age and marrow fat content on pharmacokinetic parameter values. *AJR Am J Roentgenol* 2013;**200**:W297–303.
34. Leach MO, Brindle KM, Evelhoch JL, et al. The assessment of anti-angiogenic and antivascular therapies in early-stage clinical trials using magnetic resonance imaging: issues and recommendations. *Br J Cancer* 2005;**92**:1599–610.
35. van Rijswijk CS, Hogendoorn PC, Taminiau AH, et al. Synovial sarcoma: dynamic contrast-enhanced MR imaging features. *Skeletal Radiol* 2001;**30**:25–30.
36. Khadem NR, Karimi S, Peck KK, et al. Characterizing hypervascular and hypovascular metastases and normal bone marrow of the spine using dynamic contrast-enhanced MR imaging. *AJNR Am J Neuroradiol* 2012;**33**:2178–85.
37. Chen WT, Shih TT, Chen RC, et al. Blood perfusion of vertebral lesions evaluated with gadolinium-enhanced dynamic MRI: in comparison with compression fracture and metastasis. *J Magn Reson Imaging* 2002;**15**:308–14.